Journal of Computational Physics **151,** 313–332 (1999)
Article ID jcph.1998.6172, available online at http://www.idealibrary.com on IDEAL®

Effective Computational Strategies for Determining Structures of Carcinogen-Damaged DNA

S. Broyde* and B. E. Hingerty†

**Biology Department, New York University, New York, New York 10003-5181; and †Life Sciences Division, Oak Ridge National Laboratory, Oak Ridge, Tennessee 37830-6480*

Received August 21, 1998; revised December 14, 1998

To determine three-dimensional conformations of DNA damaged by environmental chemical carcinogens, effective molecular mechanics search techniques have been developed to deal with the large system sizes and computational demands. First, extensive surveys of the potential energy surface are carried out by energy minimization. These search strategies rely on (1) using the reduced variable domain of torsion-angle (rather than Cartesian) space, (2) building larger units (about 12 base pairs) on the basis of structures of small modified subunits, and (3) employing penalty functions to search for selected hydrogen bonding patterns and to incorporate interproton distance bounds when available from experimental high-resolution nuclear magnetic resonance (NMR) studies. Second, molecular dynamics simulations with solvent can subsequently be employed to probe conformational features in the presence of polymerase enzyme responsible for DNA replication, using structures computed in the energy minimization searches as initial coordinates. A key structure–function relationship involving mirror-image molecules with very differing experimentally determined tumorigenic potencies has been deduced: the members of the pairs align oppositely when bound to DNA, making it likely that their treatment by replication and repair enzymes differ. This opposite orientation phenomenon, first predicted computationally (Singh *et al*., 1991), has been observed in experimental high-resolution NMR studies combined with our molecular mechanics computations in a number of different examples and has recently been confirmed experimentally in other laboratories as well (reviewed in Geacintov *et al*., 1997). Elucidation of this conformational feature has paved the way to uncovering the structural origin underlying very different biological outcomes stemming from chemically identical but mirror-image molecules.

Key Words: molecular mechanics; molecular dynamics; carcinogen–DNA structures.

0021-9991/99 $30.00

INTRODUCTION

The task of determining nucleic acid structures by molecular mechanics and dynamics is formidable. The large multi-dimensional surface of the potential energy must be surveyed strategically in order to locate energetically feasible structures. The multiple minimum problem is the key obstacle in the minimization quest, and the limited sampling is a severe handicap in dynamic simulations [62]. Our efforts are directed toward addressing the multiple minimum problem in the computation of DNA structures, with particular focus on DNA damaged by linkage with environmental chemicals that cause cancer. Molecular dynamics simulations are used to complement energy minimization studies, using structures from the static searches as initial ones for dynamics. This review of our work summarizes practical strategies we have devised; it also describes structural features pertaining to mutagenicity and carcinogenicity that have been uncovered, both predictive and in experimental/computational efforts with our collaborators, Dinshaw J. Patel of Memorial Sloan Kettering Cancer Center and Nicholas E. Geacintov of New York University.

Polycyclic aromatic hydrocarbons are one family of substances that we study. Ubiquitous in our environment, polycyclic aromatic hydrocarbons belong to a class of carcinogen precursor that humans are exposed to continually. They are undesirable by-products formed during combustion and hence are present in automobile exhaust, factory emissions, and tobacco smoke [36, 37, 58]. Thus, these chemicals contaminate our air, food, and water supplies. The polycyclic aromatic hydrocarbons can become chemically altered in our bodies, changing into highly reactive substances called diol epoxides [16, 37]. These diol epoxides then can bind chemically to DNA, forming joint molecular systems called carcinogen–DNA adducts. The creation of these carcinogen–DNA adducts is widely believed to be a critical initiating step in the complex carcinogenic process [57]. The adducts can cause mutations in key genes involved in regulating growth [28, 71], and these mutations can ultimately result in the formation of malignant tumors. Remarkably, the diol epoxides that result from the biological activation can have markedly different tumorigenic potentials even when they are very similar chemically [35]. This has been a subject of intense interest among workers in the field of cancer research for decades.

Benzo[a]pyrene (BP) (Fig. 1) is a polycyclic aromatic hydrocarbon that has long been studied as a paradigm for the fascinating chemical structure/tumorigenic potency relationship. In particular, benzo[a]pyrene can be biochemically altered into, among others, one pair of diol epoxides that are mirror images of each other [16]. These are known as (+)- and (−)-*anti*-benzo[a]pyrene diol epoxide (BPDE). Intriguingly, the (+)-*anti*-BPDE is tumorigenic in rodents, while the (−)-*anti*-BPDE is not [11, 68]. Both can link to DNA at the same site, the amino group of the base guanine, to form, among others, combination molecules known as the (+)- and (−)-*trans*-*anti*-[BP]-N^2-dG adducts [15, 49]. In the case of (+)-*anti* BPDE, its (+)-*trans*-*anti*-[BP]-N^2-dG adduct is the major reaction product (more than 90%) with DNA and hence is considered to be a likely culprit in the carcinogenicity of benzo[a]pyrene. The corresponding DNA adduct of the nontumorigenic (−)-*anti* BPDE is not harmful, since the parent BPDE is nontumorigenic. The structural differences between these two carcinogen–DNA adducts had been a long sought goal in the effort to understand the biological differences of these stereoisomeric molecules.

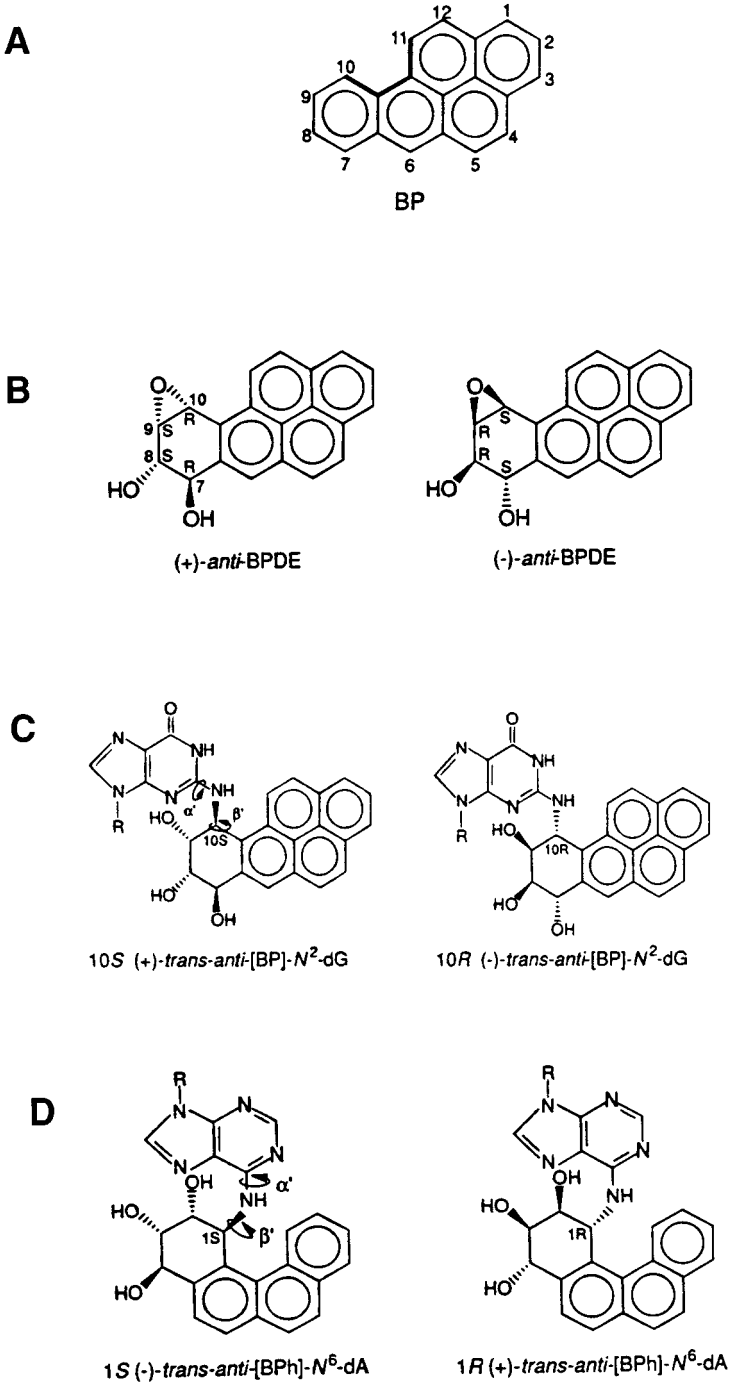

FIG. 1. (A) Benzo[a]pyrene. (B) (+)- and (−)-*anti*-BPDE. (C) (+)- and (−)-*trans-anti*-[BP]-N^2-dG adducts. R, the rest of the DNA chain, is connected to the base guanine. (D) (+)- and (−)-*trans-anti*-[BPh]-N^6-dA adducts. R, the rest of the DNA chain, is connected to the base adenine. In (C) and (D) the flexible torsion angles α' and β', governing the orientation of the polycyclic aromatic moiety with respect to the DNA, are indicated by arrows. These are defined as follows for (C): $\alpha' = $ N1(G)–C2(G)–N^2(G)–C10(BP); $\beta' = $ C2(G)–N^2(G)– C10(BP)–C9(BP).

The problem of conformational searching and sampling is a complex one, and many approaches have been developed and tailored to systems of different sizes and types. (Some important techniques are given in [2, 3, 5, 6, 38, 42, 43, 59, 65, 70, 72, 77].) In our application involving DNA linked covalently with a bulky carcinogen, the task can often be simplified to avoid searching all of conformation space because the DNA conformation, while not rigid, is usually within the family of one of the standard ones—normally the B form—but also possibly the A, Z, or their variants [60]. In this case the task reduces to searching as exhaustively as possible for feasible positions of the carcinogen. We employ molecular mechanics computations with energy minimization from multiple starting structures to perform conformational surveys and use the reduced-variable domain of torsion-angle space in the minimizations.

Our conformational searches with molecular mechanics computations have played a key role in elucidating striking structural differences in the (+)- and (−)-*trans-anti*-[BP]-N^2-dG adduct pair: an opposite orientation has been noted with respect to the DNA double helix cylinder to which the carcinogen is attached. This opposite orientation phenomenon was first predicted computationally in our work [66], and then observed experimentally in solution by high resolution nuclear magnetic resonance (NMR) experiments combined with our molecular mechanics computations [18, 27]. Moreover, numerous earlier modeling efforts (reviewed in [66]) failed to predict the opposite orientations. Recently, Kozack and Loechler [44, 45] have employed modeling by computer graphics, molecular mechanics with energy minimization, and molecular dynamics to generate structures for the (+)-*trans-anti*-[BP]-N^2-dG adduct in a number of DNA base sequences relevant to their mutagenicity studies. These structures belong to families similar to those computed in our work [66]. As far as we are aware, no other systematic large-scale conformational searching for structures of DNA damaged by covalent linkage with bulky aromatic carcinogens has been undertaken.

The opposite orientation phenomenon has now been revealed as a general principle, true for other (+) and (−) pairs of diol epoxides stemming from different polycyclic aromatic hydrocarbons whose carcinogenic potentials differ [35]. In addition, a molecular dynamics simulation for the (+)-*trans-anti*-[BP]-N^2-dG adduct in the presence of a polymerase enzyme [67] has suggested specific hydrogen-bonding interactions between the carcinogen and a key amino acid residue of the enzyme as one plausible explanation for certain mutagenic and polymerase blocking effects of the adduct.

COMPUTATIONAL APPROACH

Our molecular mechanics program, DUPLEX [41], has been tailored for investigating carcinogen–DNA adducts. DUPLEX utilizes special strategies to address the multiple minimum problem in surveying the potential energy surface, as follows (see Table 1):

(1) Internal rather than Cartesian coordinates are the minimization variables. These internal coordinates are the flexible torsion angles (i.e., rotations of groups about the bond connecting them) that describe the large movements which govern DNA shape. Torsion angles are allowed to vary over the full 360° range in our searches. Most bond lengths and bond angles, and the dihedral angles within aromatic substituents, all of which vary little in nature (a few degrees or a few tenths of an angstrom), are fixed at equilibrium values. (The puckered five-membered sugar ring requires variable bond lengths and angles, and a special pseudorotation treatment [1] to permit flexible puckering.) This representation reduces the number of variables that must be simultaneously optimized from $3N - 6$ (N, number of

TABLE 1
Practical Computational Strategies

Computational problem	Practical approach	Outcome
Large system size problem in conformational searching	Molecular representation is in internal (torsion) space (i.e., bond length, angles and most dihedral angles are fixed) rather than Cartesian space	~10 degrees of freedom per modified DNA nucleotide instead of ~180 (~60 atoms × 3) produce efficient searches
Obtaining correct geometries in conformational refinement: Chirality about atoms can be inverted and bonds broken when starting structures are high in energy in Cartesian space studies	Torsion space representation	Chirality and bonding remain as in the initial structure
Enormity of conformations in the conformational search space	Build-up strategy can be used to construct reasonable starting structures as combinations of minima of the building blocks; standard starting conformations for the DNA can also be employed	With NMR data, 16 trials per modified duplex trimer or pentamer can suffice, followed by structural embedding into a larger B-DNA duplex; without NMR data, thousands of minimization trials may be needed
Multiple minimum problem: difficulty in reliable location of correct hydrogen bonding patterns between the two DNA strands; unusual (non-Crick–Watson) base-pairing patterns are important in carcinogen/modified DNA structures.	Restraint functions aiding in location of possible hydrogen-bonding patterns are added; these are released in terminal minimizations	Conformational searching using these functions reveals possible hydrogen-bonding arrangements and their relative energies
Employing experimental NMR interproton distance data	Restraint functions are added to torsion space searches	The penalty/restraint functions guide refinement to experimentally compatible domains; atomic resolution structures are produced within the bounds of the data
Probing conformational features in presence of polymerase enzyme and explicit aqueous solvent	Cartesian space molecular dynamics simulations are used without experimental restraints	Key interactions between carcinogen and enzyme are suggested

atoms) to about 9 for a carcinogen-modified nucleotide (one base–sugar–phosphate building block). This approach is particularly suited to our interest in deducing the orientation of the carcinogen, which is largely governed by the flexible torsion angles at the carcinogen–DNA linkage site (Fig. 1). Moreover, the fixed internal coordinates have a further advantage: unrealistic internal geometries and inversions of chirality by bond breakage, a hazard in Cartesian space minimizations [43], is impossible.

(2) We have developed useful strategies for searching the large potential energy surface which cannot be sampled exhaustively by minimization techniques [39, 41, 66, 73]. Small modified subunits are constructed first. This again reduces the number of variables and is especially useful for helical DNA with carcinogen modification, where shape is governed by

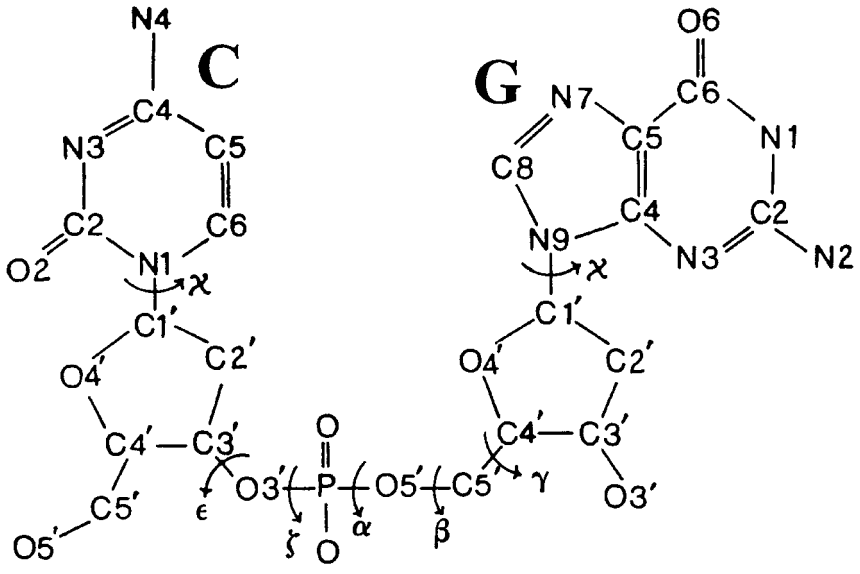

FIG. 2. Structure of the deoxynucleoside monophosphate d(CpG). C is the base cytosine, G is the base guanine. Flexible torsion angles are indicated by arrows. They involve the following atomic sequences: χ(C) = O4′–C1′–N1–C2; ε = C4′–C3′–O3′–P; ζ = C3′–O3′–P–O5′; α = O3′–P–O5′–C5′; β = P–O5′–C5′–C4′; γ = O5′–C5′–C4′–C3′; χ(G) = O4′–C1′–N9–C4. The flexible puckering of the five-membered sugar ring is represented by an additional variable, the pseudorotation parameter [1], in our torsion space energy minimization searches. The DNA chain continues at the free O5′ and O3′ in longer units. The 5′ direction is toward the free 5′–O at the left chain terminus and the 3′ direction is toward the free 3′–O at the right chain terminus. These are actually OH groups at the termini. Hydrogens have been omitted for clarity.

short-range forces. In some cases we begin with single stranded carcinogen modified dimers, with two bases and the sugar–phosphate–sugar backbone connecting them (Fig. 2), or even nucleosides containing just sugar and modified base. The dimers are conformational building blocks of the standard Watson–Crick B form of DNA containing one repeat of the DNA flexible torsions. In such small subunits we can thoroughly study both the torsion angles of the DNA backbone and those governing the carcinogen orientation, if desired. In this case, starting structures for energy minimizations can consist of about 4000 combinations of all the flexible torsion angles (39). These are selected from the known preferred torsion-angle domains for DNA subunits, together with arbitrarily positioned carcinogens whose linkage torsion angles are surveyed at a selected interval of each angle, such as 45°. In the case of the smaller nucleosides very exhaustive searches over the base–carcinogen and base–sugar torsion angles, at 5° intervals of each, in combination, are feasible [73]. Another strategy is to employ as starting structure a carcinogen-modified DNA single- or double-stranded trimer or pentamer, in a standard B-DNA conformation. Again, a large number of arbitrary, high energy carcinogen–DNA orientations are then created, employing torsion-angle values for the carcinogen–DNA linkage which divide each 360° torsion space into fourths, eighths or sixteenths, in combination. A finer pattern of conformational space searching, and hence a larger number of trials, is needed when no experimental NMR data are available. Low-energy structures from these searches can be embedded into larger B-DNA duplexes with subsequent energy minimization to yield energy-ranked structures.

(3) Penalty functions added to the energy can be employed as searching tools to aid the minimization algorithm in locating structures on the potential energy surface. A hydrogen

bond penalty function [41] is used to search for any selected hydrogen-bonding pattern between chosen hydrogen bond donor–acceptor pairs. This function is particularly useful for carcinogen-damaged DNA which may have unusual hydrogen-bonding patterns different from the normal Watson–Crick pairing (i.e., adenine/thymine (A/T), and cytosine/guanine (C/G)). Carcinogen-induced denaturation (i.e., disruption of hydrogen bonding between normally Watson–Crick base-paired partners) may also be sought with this function by omitting its use at the designated site. In addition, penalty functions are employed to incorporate experimentally measured interproton distances in the searches [19, 35, 61], when they are available from high-resolution NMR data; experimental solution studies are carried out in the laboratory of our collaborator, Dinshaw J. Patel, at Memorial Sloan Kettering Cancer Center with carcinogen-modified DNAs synthesized in the laboratory of our collaborator, Nicholas E. Geacintov, at New York University. In this case, structures in agreement with the NMR data can be achieved very rapidly, with only a small number of trials needed, often just 16, to locate about 4 that are within the range of the experimental data (i.e., between the upper and lower interproton distance bounds). A judicious choice of penalty-function weights, developed with experience, is key to ensuring convergence by this approach. Both the NMR data and the intrinsic energies are allowed to play a part. Moreover, in cases where there is conformational mobility with attendant uncertainty in interpreting some aspects of the NMR data, a first set of computed structures can provide feedback to the NMR researchers; this offers the opportunity to provide revised distance bounds for a subsequent set of trials. Again, the subunits employed in the searches can be built to larger duplexes by embedding the smaller carcinogen modified subunit in a larger B–DNA duplex, which is then minimized. In a terminal minimization, all penalty functions are released to yield final structures that are unrestrained minimum energy conformations.

When NMR data are available, the final structures obtained from DUPLEX can be refined further by conventional Cartesian space molecular dynamics/simulated annealing approaches, such as are available in the XPLOR package [8, 10]. (NMR refinement techniques are reviewed in [7, 9, 12].) See also [62] for an overview of dynamics as well as refinement techniques. Small adjustments in bond lengths, bond angles, and dihedral angles occur at this stage, which is achieved rapidly because of the high-quality initial structure.

The force field employed by DUPLEX employs standard potential energy functions developed for nucleic acids [52]. (See also [14, 46] for reviews of nucleic acid force fields and modeling.) Full details of the force field and parametrization have been published (41). The potentials include the important Lennard–Jones, Coulombic, and torsional terms (see the Appendix), as well as special terms required to reproduce nucleic acid conformational [51, 69] and hydrogen-bonding [50] preferences. The energy is computed with no distance-dependent cutoff. Counterion condensation to neutralize the negative charge of the DNA phosphodiester backbone at neutral pH can be mimicked by reduced partial charges on the pendant phosphate oxygens, or by explicit metal ions [40, 46]. Solvent is modeled by distance-dependent dielectric functions (40, 46, 52). A selected counterion concentration, typically 0.1 M monovalent cation, can be included in the dielectric screening term [32]. Atomic partial charges for the carcinogen, required for the Coulombic term, are computed with the same quantum mechanical semi-empirical method which derived the nucleic acid charges [53]. Barriers to rotation about the bonds linking the carcinogen to the DNA are taken from experimental values for small molecules containing chemically similar linkages or from quantum mechanical calculations.

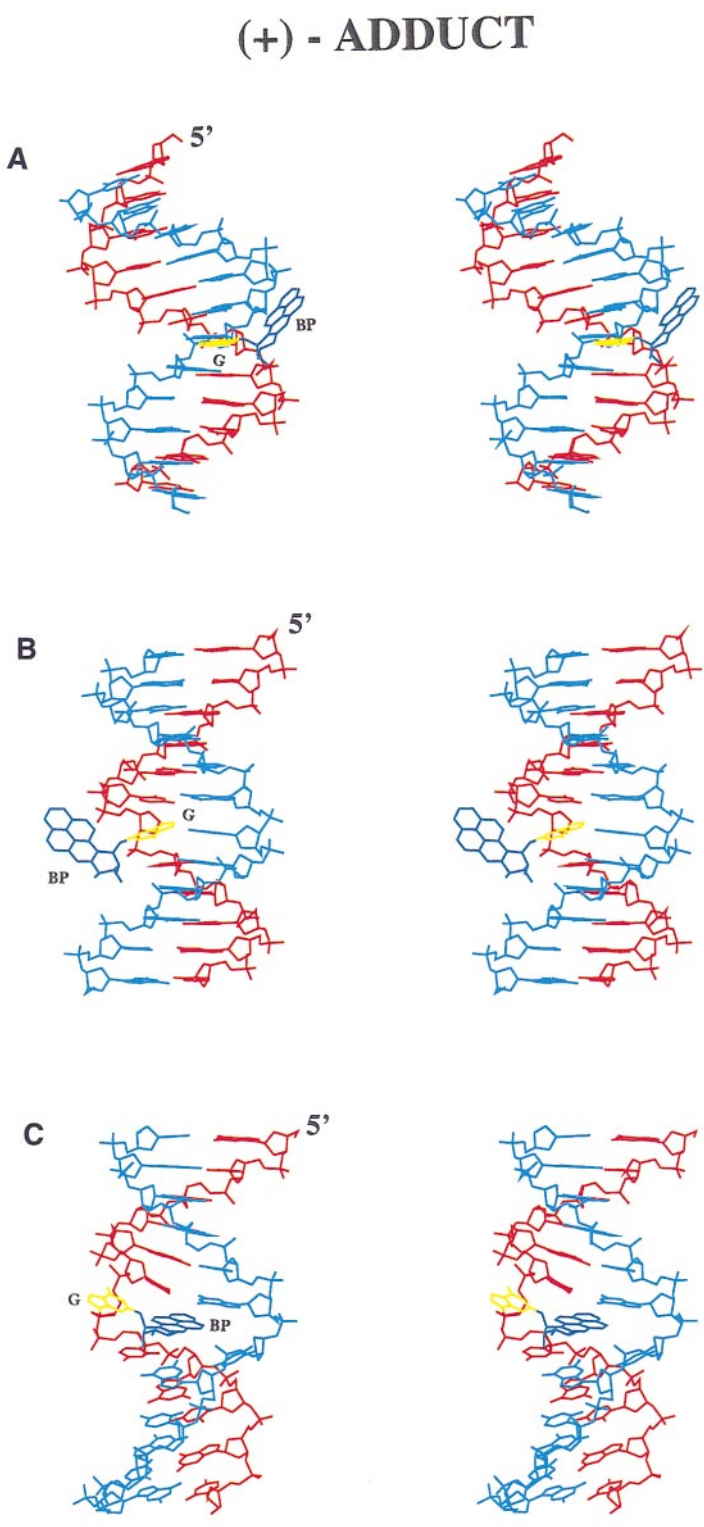

FIG. 3. Stereo views of three structural types computed for (+)- and (−)-*trans-anti*-[BP]-N^2-dG adducts. Left panel: (+) adduct. Right panel: (−) adduct. BP in (A) minor groove position; minor groove is on the right; (B) major groove position; major groove is on the left; (C) Base displaced–intercalated position; major groove is in front, minor groove is in back. Hydrogens have been omitted for clarity. The unmodified DNA strand is cyan, the modified strand is red, the modified guanine is yellow, and the carcinogen is dark blue. The 5′ end of the modified strand is designated.

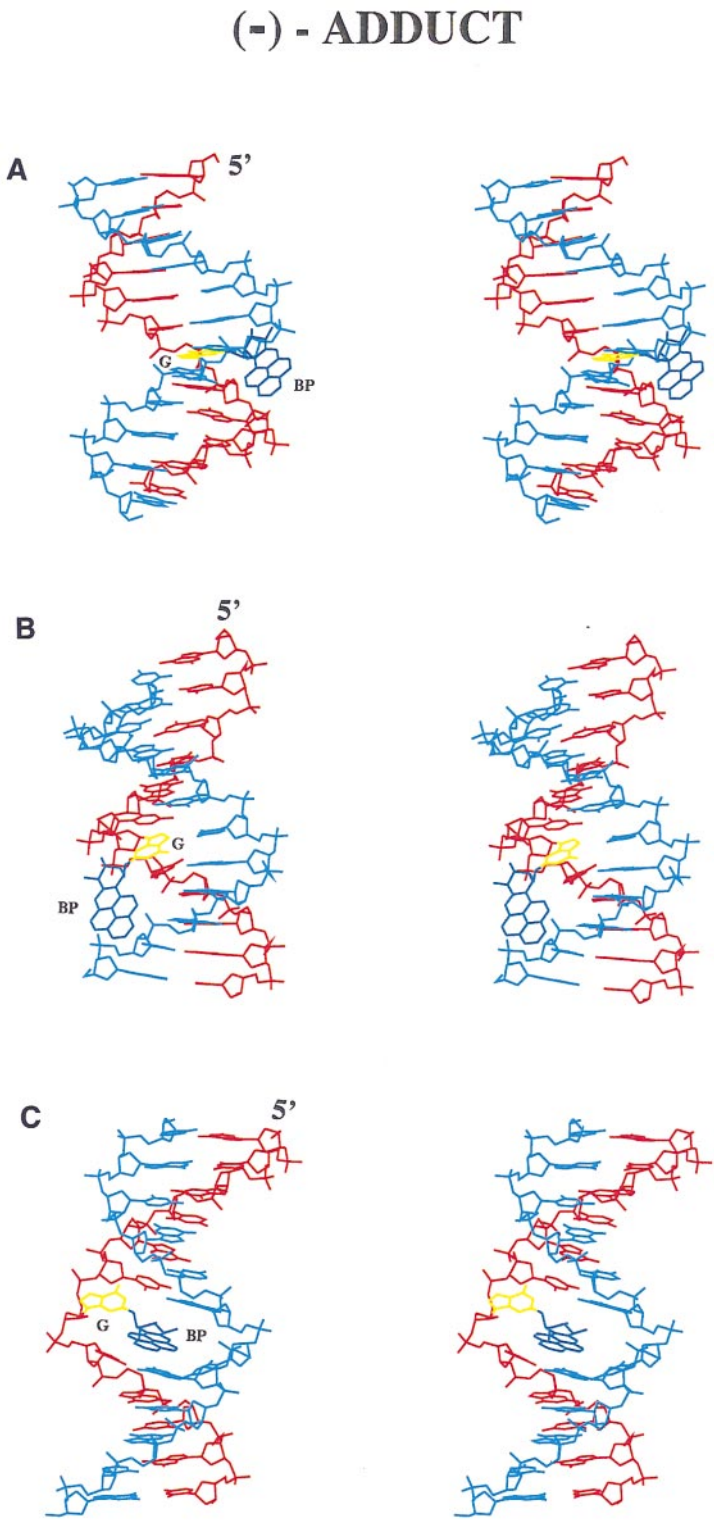

FIG. 3—*Continued*

Low-energy structures computed in the static searches then can serve as initial structures in molecular dynamics simulations containing polymerase enzyme and explicit aqueous solvent. We used AMBER 4.0 [55] for this purpose [67] prior to release of AMBER 4.1 with the Cornell *et al*. force field [17] and the particle mesh Ewald treatment for electrostatic interactions [26]; currently we employ AMBER 5.0 with these enhancements. (A review of nucleic acid molecular dynamics simulation is given in [3].)

Computations are performed at the Department of Energy's National Energy Research Supercomputer Center and the National Science Foundation's San Diego Supercomputer Center, utilizing the Cray C90 machines. A set of 16 energy minimization trials for a carcinogen modified DNA duplex pentamer takes about 6 CPU hours on the Cray C90. A single energy minimization trial for a duplex dodecamer takes about 10 CPU hours. These calculations can be completed in about 2 days (depending on machine load and run priority selected). The dynamics simulation with carcinogen-modified DNA, polymerase enzyme, and solvent (about 12,000 atoms) was mainly performed on an SGI Challenge XL workstation at Wyeth Ayerst Research Laboratories. A picosecond took about 1 day of CPU time on that machine.

RESULTS AND DISCUSSION

Our original studies for the two BPDE adducts of Fig. 1C employed no experimental information other than the force field parameters. About 4000 energy minimization trials were first performed for a modified deoxydinucleoside monophosphate d(CpG) [39]. About 300 additional trials were carried out for the modified single-stranded trimer d(CpGpC), and about 100 further trials were carried out with modified duplex trimers. Finally, low-energy conformers located from the searches were embedded in duplex dodecamers in the base sequence $d(GC)_6 \cdot d(GC)_6$, with carcinogen modification at the fourth G [66].

A remarkable universal distinction between the (+) and the (−) adduct structures emerged from these conformational searches: regardless of the specific type of orientation with respect to the DNA adopted by the benzo[a]pyrenyl moiety, it was always oppositely aligned in the two stereoisomers. (The (+) and (−) DNA adducts are stereoisomers, but not enantiomers—mirror images—like the BPDE reactants, because the DNA molecules are not mirror images.) Three structural classes were computed. In one structural type the benzo[a]pyrenyl ring system is situated in the B-DNA minor groove, at the helix exterior (Fig. 3A). However, the DNA double helix has directionality, since it is not symmetric. The directions are termed 5′ and 3′ (see Fig. 2). In the (+) case the benzo[a]pyrenyl rings are pointing in the 5′ direction of the damaged strand, while they are pointing 3′ in the (−) case. In a fixed view of the DNA, this can be described as pointing up or pointing down. The second class also involves the helix exterior, but the major rather than the minor groove. In this class the benzo[a]pyrenyl rings are situated on the opposite face of the double helix cylinder from the minor groove, i.e., the major groove. Again, the (+) adduct has the pyrene ring system directed 5′ along the modified strand and the (−) adduct has the pyrene rings pointing in the 3′ direction (Fig. 3B). The third computed orientation is termed base-displaced intercalation. It involves removal of the modified guanine from its stacked position within the helix so as to make room for the benzo[a]pyrenyl system, which is now stacked between adjacent base pairs in its stead (Fig. 3C). Interestingly, even in this case the orientation is opposite in the (+)/(−) pair, but with respect to the major versus minor groove sides of the helix cylinder. As shown in Fig. 1C, the BP moiety contains four planar aromatic rings as well as a ring containing three OH groups linked to guanine. This latter

ring is puckered. In the (+) adduct case the BP planar aromatic ring most distant from the linkage site to guanine is on the *minor* groove side, and the puckered near ring containing the OH groups is on the major groove side of the helix cylinder; in the (−) case the distant planar aromatic ring is on the opposite, *major* groove side, and the OH group-containing puckered ring is on the minor groove side.

Experimental synthesis and high-resolution NMR studies combined with our molecular mechanicscalculations were carried out subsequently, in collaboration with the Geacintov and Patel laboratories. These involved DNA duplexes containing the (+)- and (−)-*anti*-BPDE adducts, in different base sequence contexts from those employed in our predictive computations. Both the minor groove and the base-displaced intercalation orientations have now been observed in these solution studies (in two different base sequence contexts), and

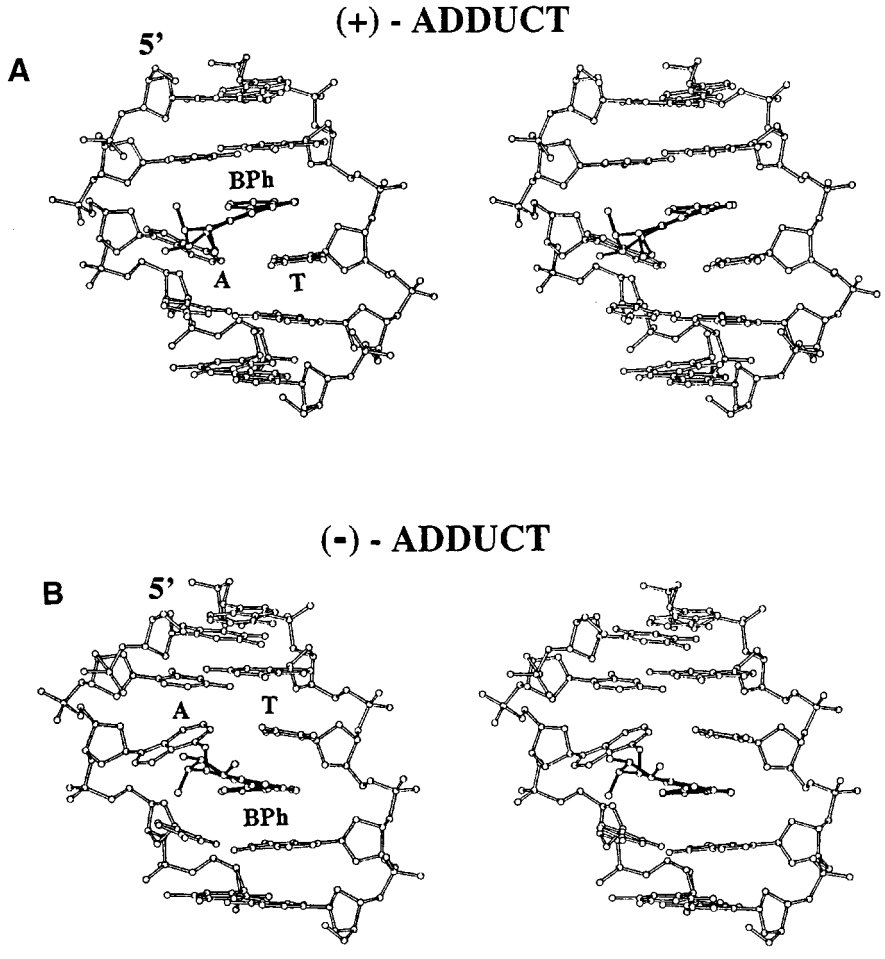

FIG. 4. Stereo views of (A) (+)- and (B) (−)-*trans*-*anti*-[BPh]-N^6-dA adducts intercalated on the 5′ and 3′ sides of the modified base adenine (A) and its partner thymine (T), respectively; structures were obtained by experimental high-resolution NMR studies together with molecular mechanics computations [9, 10]. The central 5-mer of the 11-mer duplex is shown. Hydrogens are deleted for clarity. The designated A:T pairs contain distorted hydrogen bonds characterized by propeller twists and buckles of 15° and −30°, respectively, in the (+) adduct, and −23° and 32°, respectively, in the (−) adduct, computed with the algorithm of Babcock and Olson [4]. Ideal B-DNA values are 0°. The 5′ end of the modified strand is designated.

the opposite orientation phenomenon has been observed exactly as predicted in all four cases [18, 21, 27, 31, 35].

The origin of the opposite orientation effect has recently been investigated through extensive molecular mechanics surveys of the potential energy surface of a (+)/(−) adduct pair in a simple nucleoside containing just a BP-adducted guanine together with its attached sugar, involving 373,248 structures for each adduct. These studies revealed that the opposite orientation effect is manifest even in BP-modified nucleosides and that simple steric hindrance is responsible for the phenomenon [73]. When the benzo[a]pyrenyl moiety in the (+) case is rotated to a domain favored by the (−) adduct, and vice versa, crowded structures are produced. The crowding stems from the differing positions of the OH groups and the linkage to guanine in the two benzo[a]pyrenyl adducts (Fig. 1). Thus, the mirror-image nature of the BP moiety in the (+) and (−) adducts produces such forceful steric effects that they are retained in DNA duplexes.

The predictions and observations of opposite orientations for the (+)- and (−)-*anti*-BPDE adducts have proved to be a general principle. NMR solution studies with molecular mechanics/dynamics computations, both from our collaboration with the Patel and Geacintov laboratories and from other laboratories, have now elucidated solution structures of a number of different DNA adducts from (+) and (−) pairs of diol epoxides. These are derived from various aromatic hydrocarbons, with differing numbers and positioning of aromatic rings, and with differing carcinogenic potencies, bound to the base guanine or adenine [18–25, 27, 29–31, 34, 47, 48, 63, 64, 74–76] (reviewed in [35]). The positions adopted include the three types computed for the (+)- and (−)-*trans-anti*-[BP]-N^2-dG adducts. In addition, a fourth theme has been observed: classical intercalation, in which the polycyclic aromatic rings are inserted into the double helix *without* displacement of the modified base; stretching and unwinding the helix makes room for the carcinogen. This theme has been observed for the adenine adducts. However, it is quite striking that regardless of the conformational theme adopted, the specific polycyclic compound, and the base modified, the

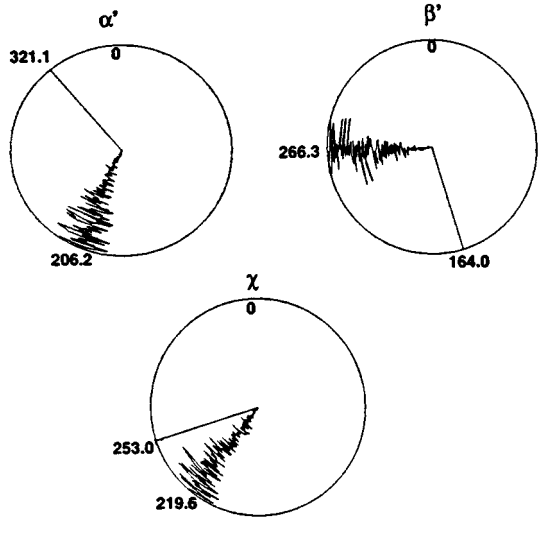

FIG. 5. Mobility of BP moiety and modified G4 as manifested in torsion angle dynamics of α', β', and χ in degrees. The radius of the circle is the time axis with 0 ps at the center and 200 ps at the circumference. Values for the starting structure are designated by nonfluctuating radii. Average and starting values are given on the circumference.

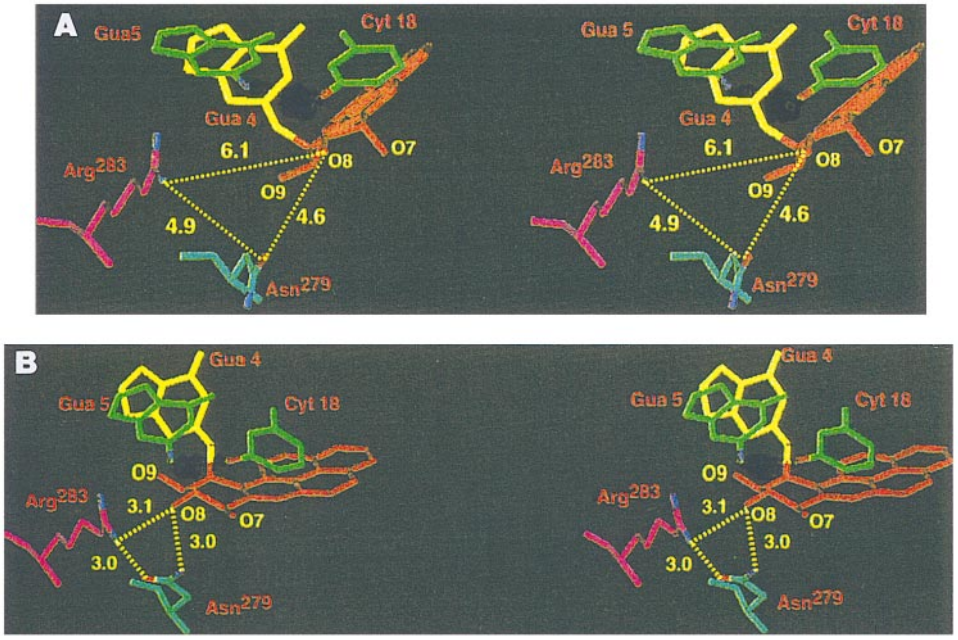

FIG. 6. Stereo views from molecular dynamics simulation of (+)-*trans-anti*-[BP]-N^2-dG adduct at a primer/template junction within the rat β polymerase enzyme (Singh *et al.*, 1998). Key hydrogen bonding interactions are denoted. The BP moiety is red. Hydrogens have been omitted for clarity.

members of the (+)/(−) pair are oriented oppositely in the DNA in all examples observed so far. In the case of classical intercalation involving the adenine adducts, this opposite orientation effect is manifested by insertion of the aromatic rings on the 5′ side of the modified base (which remains paired with its partner via distorted Watson–Crick hydrogen bonds) in the (+) adduct, and on the 3′ side in the (−) adduct. (One can view this as above or below the modified base and its partner.) Figure 4 shows this conformational theme for the (+)/(−) pair of benzo[c]phenanthrenyl (PBh) adducts to adenine (Fig. 1D). Benzo[c]phenanthrene is another environmental polycyclic aromatic hydrocarbon that is biochemically activated to mirror-image diol epoxides with differing tumorigenic potencies. These molecules link predominantly to the adenine bases of DNA (see [35] for review).

The next step in our computations is to include replicative or repair enzymes in the molecular mechanics and dynamics simulations. This is important because carcinogen-damaged DNAs interact with these enzymes in the biological context of the cell. A beginning has been made in this direction. With Suresh B. Singh, now at Merck Research Laboratories, and in collaboration with the laboratory of Samuel H. Wilson at NIEHS, we conducted a molecular dynamics simulation of a model containing replicating DNA (termed a primer/template complex) within a replicating enzyme, rat β polymerase [67]. The base sequence studied was

5′-d(A1–A2–A3–G4–G5–G6–C7–G8–C9–C10–G11)-3′-parent

3′-d(C18–C17–G16–C15–G14–G13–C12)-5′-daughter

The parent strand contains residues 1–11, and the newly synthesized daughter strand contains residues 12–18; hence, G4 is next to be replicated. Coordinates from the crystal structures of this primer/template complex within the polymerase provided the starting

TABLE 2
Hydrogen Bonding in Dynamics Simulation

Hydrogen bond	Average distance (Å)	Standard deviation (Å)	Average angle (°)	Standard deviation (°)
Arg^{283} NH · · · O8[BP]	3.0 (6.1)	0.3	145.8	18.4
Asn^{279} NH · · · O8[BP]	3.1 (6.1)	0.6	173.2	13.5
Arg^{283} NH · · · N[Asn^{279}]	3.7 (6.1)	0.5	175.8	8.6
Arg^{283} NH · · · O[Asn^{279}]	2.9 (4.9)	0.4	168.5	16.6

Note. Averaged over first 200 ps. Hydrogen bonds have begun to form by 3 ps and are stable by 15 ps. Values for starting structure are given in parentheses. Distances are from heavy atom to heavy atom. Starting hydrogen bond angles were not measured since the hydrogen bonds were absent.

coordinates for the enzyme and the DNA except for G4 [56]. Base G4 was modified to form the (+)-*trans-anti*-[BP]-N^2-dG adduct, positioned in the minor groove directed 5′ along the modified strand, as obtained in our computations [66] and in the combined experimental/computational work [18]. The total system of 12,249 atoms included 2,163 water molecules. Counterions were not employed since the DNA was in contact with neutralizing positively charged amino acid residues. Energy minimizations and molecular dynamics simulations for 225 ps were performed using AMBER 4.0 [55], with the protocol described in Singh *et al*. [67]. A biologically very significant rearrangement was captured in this time frame: the carcinogen and its attached G4 realigned within the first 15 ps of the simulation and then remained stably positioned. In particular, the G4 became less stacked with the G5–C18 base pair while the benzo[a]pyrenyl moiety shifted so it is somewhat stacked with C18. This motion caused the critical Watson–Crick hydrogen bonding edge of the templating G4 to be partly obstructed by the carcinogen. The carcinogen–base torsion angles α' and β' responsible for this motion shifted from starting values of 321.1° and 164.0°, respectively, to average values of 206.2° +/−11.6° and 266.3° +/−10.7°, respectively (Fig. 5). Concomitant with this motion, critical new hydrogen bonds were formed (Table 2 and Fig. 6). These involved the carcinogen and key amino acid residues of the polymerase, Arg^{283} and Asn^{279}. Arg^{283} plays an essential role in polymerase fidelity and efficient catalysis [5] by stabilizing the position of the templating G4 [56]. Asn^{279} stabilizes the position of the incoming partner to G4 [56]. The formation of hydrogen bonds both between these critical amino acid residues, and between each of them and the carcinogen, together with the shifted position of the templating G4, would compromise the enzyme's capability for faithful and efficient nucleotide incorporation. The predominant observed biological effect of the (+)-*trans-anti*[BP]-N^2-dG adduct in DNA replication studies (reviewed in [35, 54, 67]) is polymerase blockage, or misincorporation of adenine opposite the lesion, when the blockage is overcome. Substitution of alanine for the critical Arg^{283} in the polymerase causes a marked reduction in fidelity and catalytic efficiency together with a strong tendency to induce G · A mispairing [5], in line with the effects induced by the (+)-*trans-anti*-[BP]-N^2-dG adduct.

While a different force field, a different dynamics protocol, or a different force field treatment for electrostatics [26, 33] could yield a different type of structure, the first biological understanding at a molecular level of one plausible mechanism for mutagenic and polymerase blocking effects of the benzo[a]pyrenyl moiety was realized from this simulation.

CONCLUSION

The observed striking opposite orientation effect which was computationally predicted is one reasonable underpinning behind the differing biological outcomes produced by (+) and (−) diol epoxide pairs; the enzymes that interact with the lesions during DNA replication and repair would respond differently to the opposite orientations if the phenomenon also occurred under the biological conditions of the cell. Since the underlying origin of the opposite orientations is steric, it is not unlikely that it would remain manifest even under the complex cell conditions. Thus, this work has paved the way for the possibility of uncovering basic structural origins underlying very different biological outcomes from chemically very similar, even mirror image molecules. One of our goals is to develop a library of structural hallmarks associated with observed mutagenicity and carcinogenicity for a large number of substances. Molecular mechanics and dynamics computations by themselves, and in combination with high-resolution NMR data if available from collaborators, are playing an important role in developing this database. Improved computational techniques and faster computers are crucial for handling successfully large biological systems, especially for probing their rich range of dynamic flexibility, key to biological function. Ultimately, one hopes to computationally predict which substances are harmful and which are benign. This would avoid the laborious, expensive, and controversial tests of mammals that are now necessary to identify carcinogenic substances present in the environment. Of course, deep understanding of the complex, multi-stage process of carcinogenesis (57) will be required to achieve this aim.

APPENDIX

The potential energy function in the torsion-angle space program DUPLEX contains only nonbonded force field terms since bond lengths, bond angles, and most dihedral angles are invariant. The predominant terms are the following:

(1) A Lennard–Jones 6–12 potential describes the Van der Waals interaction between atoms i and j separated by a distance r:

$$E_{\mathrm{VDW}} = -a_{ij}r^{-6} + b_{ij}r_{ij}^{-12}.$$

The first term represents the attractive dispersion interaction and the second the repulsive steric interaction; a and b are parameters chosen to achieve a minimum in the energy function near the sum of the Van der Waals radii.

(2) A Coulomb potential accounts for electrostatic contributions to the nonbonded energy

$$E_{\mathrm{elec}} = \frac{q_i q_j}{\varepsilon r_{ij}},$$

where the q's are partial charges and ε is the dielectric constant of the medium.

(3) A torsional potential accounts for energetics of twisting 1–4 atoms (in a bonded quadruplet sequence) about the bond formed by atoms 2 and 3:

$$E_{\mathrm{tor}} = \mathrm{Vo}/2(1 \pm \cos(m\theta)).$$

The function form is selected to reproduce the phase, periodicity, and amplitude suitable to

the particular chemical bond about which the rotation takes place, via the integer m, and appropriate choice of sign and Vo, the barrier height. θ is the flexible torsion angle.

ACKNOWLEDGMENTS

This research is supported by NIH Grants CA28038, CA75449, and RR06458 and DOE Grant DE-FG02-90ER60931 (S.B.), and DOE Contract DE-AC05-96OR22464 with Lockheed Martin Energy Research (B.E.H.). We thank Tamar Schlick for much helpful advice in the preparation of this manuscript.

REFERENCES

1. C. Altona and G. Sundaralingam, Conformational analysis of the sugar ring in nucleosides and nucleotides: A new description using the concept of pseudorotation, *J. Am. Chem. Soc*. **94**, 8205 (1972).
2. A. Amadei, A. B. M. Linssen, B. L. Degroot, D. M. F. van Aalten, and H. J. C. Berendsen, An efficient method for sampling the essential subspace of proteins, *J. Biomol. Struct. Dynam*. **13**, 615 (1996).
3. P. Auffinger and E. Westhof, Molecular dynamics: Simulations of nucleic acids, in *The Encyclopedia of Computational Chemistry*, edited by P. v. R. Schleyer, N. L. Allinger, T. Clark, J. Gasteiger, P. A. Kollman, H. F. Schaefer III, and P. R. Schreiner (Wiley, Chichester, 1998), Vol. 3, p. 1629.
4. M. Babcock, E. P. D. Pednault, and W. K. Olson, Nucleic acid structure analysis: Mathematics for local cartesian and helical structure parameters that are truly comparable between structures, *J. Mol. Biol*. **237**, 125 (1994).
5. W. A. Beard, W. P. Osheroff, R. Prasad, M. R. Sawaya, M. Jaju, T. G. Wood, J. Kraut, T. A. Kunkel, and S. H. Wilson, Enzyme–DNA interactions required for efficient nucleotide incorperation and discrimination in human DNA polymerase β, *J. Biol. Chem.* **271**, 12141 (1996).
6. B. J. Berne and J. Straub, Novel methods of sampling phase space in the simulation of biological systems, *Curr. Op. Struct. Biol*. **7**, 181 (1997).
7. M. Billeter, Macromolecular structures determined using NMR data, in *The Encyclopedia of Computational Chemistry*, edited by P. v. R. Schleyer, N. L. Allinger, T. Clark, J. Gasteiger, P. A. Kollman, H. F. Schaefer III, and P. R. Schreiner (Wiley, Chichester, 1998), Vol. 3, p. 1535.
8. A. Brunger, *X-PLOR User Manual* (Yale University, New Haven, CT, 1992), Version 3.1.
9. A. T. Brunger and L. M. Rice, Macromolecular structure calculation and refinement by simulated annealing: Methods and applications, in *The Encyclopedia of Computational Chemistry*, edited by P. v. R. Schleyer, N. L. Allinger, T. Clark, J. Gasteiger, P. A. Kollman, H. F. Schaefer III, and P. R. Schreiner (Wiley, Chichester, 1998), Vol. 3, p. 1525.
10. A. T. Brunger, P. D. Adams, G. M. Clore, W. L. Delano, P. Gros, R. W. Grosse-Kunstleve, J.-S. Jiang, J. Kuszewski, M. Nilges, N. S. Pannu, R. J. Read, L. M. Rice, T. Simonson, and G. L. Warren, Crystallography and NMR system: A new software suite for macromolecular structure determination, *Acta Crystallogr. D* **54**, 905 (1998).
11. M. K. Buening, P. G. Wislocki, W. Levin, H. Yagi, D. R. Thakker, H. Akagi, M. Koreeda, D. M. Jerina, and A. H. Conney, Tumorigenicity of the optical enantiomers of the diastereomeric benzo[a] pyrene 7,8-diol-9,10-epoxides in newborn mice: Exceptional activity of (+)-7b,8a-dihydroxy-9a,10a-epoxy-7,8,9,10-tetrahydrobenzo[a]pyrene, *Proc. Natl. Acad. Sci. USA* **75**, 5358 (1978).
12. D. A. Case, D. A. Pearlman, J. W. Caldwell, T. E. Cheatham, W. S. Ross, C. Simmerling, T. Darden, K. M. Merz, R. V. Stanton, A. Cheng, J. J. Vincent, M. Crowley, D. M. Ferguson, R. Radner, G. L. Seibel, U. C. Singh, P. Weiner, and P. A. Kollman, *AMBER 5.0 Documentation* (University of California, San Francisco, 1997).
13. D. A. Case, NMR refinement, in *The Encyclopedia of Computational Chemistry*, edited by P. v. R. Schleyer, N. L. Allinger, T. Clark, J. Gasteiger, P. A. Kollman, H. F. Schaefer III, and P. R. Schreiner (Wiley, Chichester, 1998), Vol. 3, p. 1866.
14. P. Cieplak, Nucleic acid force fields, in *The Encyclopedia of Computational Chemistry*, edited by P. v. R. Schleyer, N. L. Allinger, T. Clark, J. Gasteiger, P. A. Kollman, H. F. Schaefer III, and P. R. Schreiner (Wiley, Chichester, 1998), Vol. 3, p. 1922.

15. S. C. Cheng, B. D. Hilton, J. M. Roman, and A. Dipple, DNA adducts from carcinogenic and noncarcinogenic enantiomers of benzo[a]pyrene dihydrodiol epoxide, *Chem. Res. Tox.* **2**, 334 (1989).

16. A. H. Conney, Induction of microsomal enzymes by foreign chemicals and carcinogenesis by polycyclic aromatic hydrocarbons, *Cancer Res*. **42**, 4875 (1982).

17. W. D. Cornell, P. Cieplak, C. I. Bayly, I. R. Gould, K. M. Merz Jr., D. M. Ferguson, D. C. Spellmeyer, T. Fox, J. W. Caldwell, and P. A. Kollman, A second generation force field for the simulation of proteins, nucleic acids, and organic molecules, *J. Am. Chem. Soc*. **117**, 5179 (1995).

18. M. Cosman, C. de los Santos, R. Fiala, B. E. Hingerty, V. Ibanez, L. A. Margulis, D. Live, N. E. Geacintov, S. Broyde, and D. J. Patel, Solution conformation of the major adduct between the carcinogen (+)-*anti*-benzo[a]pyrene diol epoxide and DNA, *Proc. Natl. Acad. Sci. USA* **89**, 1914 (1992).

19. M. Cosman, C. de los Santos, R. Fiala, B. E. Hingerty, V. Ibanez, E. Luna, R. G. Harvey, N. E. Geacintov, S. Broyde, and D. Patel, Solution conformation of the (+)-*cis-anti*-[BP]dG adduct in a DNA duplex: intercalation of the covalently attached benzo[a]pyrenyl ring into the helix and displacement of the modified deoxyguanosine, *Biochemistry* **32**, 4145 (1993).

20. M. Cosman, R. Fiala, B. Hingerty, A. Laryea, H. Lee, R. G. Harvey, S. Amin, N. E. Geacintov, S. Broyde, and D. Patel, Solution conformation of the (+)-*trans-anti*-[Bph]dA adduct opposite dT in a DNA duplex: Intercalation of the covalently attached benzo[c]phenanthrene to the 5′-side of the adduct site without disruption of the modified base pair, *Biochemistry* **32**, 12488 (1993).

21. M. Cosman, R. Fiala, B. E. Hingerty, S. Amin, N. E. Geacintov, S. Broyde, and D. J. Patel, Solution conformation of the (+)-*trans-anti*-[BP]dG adduct opposite a deletion site in a DNA duplex: Intercalation of the covalently attached benzo[a]pyrene into the helix with base displacement of the modified deoxyguanosine into the major groove, *Biochemistry* **33**, 11507 (1994).

22. M. Cosman, R. Fiala, B. E. Hingerty, S. Amin, N. E. Geacintov, S. Broyde, and D. J. Patel, Solution conformation of the (+)-*cis-anti*-[BP]dG adduct opposite a deletion site in a DNA duplex: Intercalation of the covalently attached benzo[a]pyrene into the helix with base displacement of the modified deoxyguanosine into the minor groove, *Biochemistry* **33**, 11518 (1994).

23. M. Cosman, R. Xu, B. E. Hingerty, S. Amin, R. G. Harvey, N. E. Geacintov, S. Broyde, and D. J. Patel, Solution conformation of the (−)-*trans-anti*-[MC]dG adduct opposite dC in a DNA duplex: DNA bending associated with wedging of the methyl group of 5-methylchrysene to the 3′-side of the modification site, *Biochemistry* **34**, 6247 (1995).

24. M. Cosman, A. Laryea, R. Fiala, B. E. Hingerty, S. Amin, N. E. Geacintov, S. Broyde, and D. J. Patel, Solution conformation of the (−)-*trans-anti*-[BPh]dA opposite dT adduct in a DNA duplex: Intercalation of covalently attached benzo[c]phenanthrenyl residue to the 3′-side of the adduct site and comparison with the (+)-*trans-anti*-[BPh]dA opposite dT, *Biochem*. **34**, 1295 (1995).

25. M. Cosman, B. E. Hingerty, N. Luneva, S. Amin, N. E. Geacintov, S. Broyde, and D. J. Patel, Solution conformation of the (−)-*cis-anti*-benzo[a]pyrenyl-dG adduct opposite dC in a duplex: Intercalation of the covalently attached BP ring into the helix with base displacement of the modified deoxyguanosine into the major groove, *Biochemistry* **35**, 9850 (1996).

26. T. Darden, D. York, and L. G. Pedersen, Particle mesh Ewald: An N log(N) method for Ewald sums in large systems, *J. Chem. Phys*. **98**, 10089 (1993).

27. C. de los Santos, M. Cosman, B. E. Hingerty, V. Ibanez, L. A. Margulis, N. E. Geacintov, S. Broyde, and D. J. Patel, Influence of benzo[a]pyrene diol epoxide chirality on solution conformations of DNA covalent adducts: The (−)-*trans-anti*-[BP]GBC adduct structure and comparison with the (+)-*trans-anti*-enantiomer, *Biochemistry* **31**, 5245 (1992).

28. M. F. Denissenko, A. Pao, M.-S. Tang, and G. P. Pfeifer, Preferential formation of benzo[a]pyrene adducts at lung cancer mutational hotspots in *P53*, *Science* **274**, 430 (1996).

29. B. Feng, L. Zhou, C. M. Passarelli, and M. P. Stone, Major groove (R)-α-(N^6-adenyl)styrene oxide adducts in oligodeoxynucleotide containing human N-*ras* codon 61 sequence: Conformation of the R(61, 2) and R(61, 3) sequence isomers from ^{1}H NMR, *Biochemistry* **34**, 14021 (1996).

30. B. Feng, M. Voehler, L. Zhou, C. M. Passarelli, and M. P. Stone, Major groove S-α-(N^6-adenyl)-styrene oxide adducts in an oligodeoxynucleotide containing the human N-*ras* codon 61 sequence: Conformations of the S(61, 2) and S(61, 3) sequence isomers from ^{1}H NMR, *Biochemistry* **34**, 14037 (1996).

31. B. Feng, A. Gorin, A. Kolbanovskiy, B. E. Hingerty, N. E. Geacintov, S. Broyde, and D. J. Patel, Solution conformation of the (−)-*trans-anti*-[BP]dG adduct opposite a deletion site in a DNA duplex: Intercalation of the covalently attached benzo[a]pyrene into the helix with base displacement of the modified deoxyguanosine into the minor groove, *Biochemistry* **45**, 13780 (1997).
32. M. O. Fenley, G. S. Manning, and W. K. Olson, Approach to the limit of counterion condensation, *Biopolymers* **30**, 1191 (1990).
33. M. O. Fenley, W. K. Olson, K. Chua, and A. H. Boschitsch, Fast adaptive multipole method for computation of electrostatic energy in simulations of polyelectrolyte DNA, *J. Comp. Chem.* **17**, 976 (1996).
34. M. A. Fountain and T. R. Krugh, Structural characterization of a (+)-*trans-anti*-benzo[a]pyrene–DNA adduct using NMR, restrained energy minimization, and molecular dynamics, *Biochemistry* **34**, 3152 (1995).
35. N. E. Geacintov, M. Cosman, B. E. Hingerty, S. Amin, S. Broyde, and D. J. Patel, NMR solution structures of stereoisomeric covalent polycyclic aromatic carcinogen–DNA adducts: Principles, patterns and diversity, *Chem. Res. in Toxicology* **10**, 111 (1997).
36. G. Grimmer, Relevance of polycyclic aromatic hydrocarbons as environmental carcinogens, in *Proc. 13th Int. Symp. Polynuclear Aromatic Hydrocarbons*, edited by P. Garrigues and M. Lamotte (Gordon and Breach, Langhorne, PA, 1993), p. 31.
37. R. G. Harvey, *Polycyclic Aromatic Hydrocarbons: Chemistry and Carcinogenicity* (Cambridge Univ. Press, Cambridge, UK, 1991).
38. M.-H. Hao and H. A. Scheraga, Conformational sampling, in *The Encyclopedia of Computational Chemistry*, edited by P. v. R. Schleyer, N. L. Allinger, T. Clark, J. Gasteiger, P. A. Kollman, H. F. Schaefer III, and P. R. Schreiner (Wiley, Chichester, 1998), Vol. 1, p. 552.
39. B. E. Hingerty and S. Broyde, Carcinogen–base stacking and base–base stacking in dCpdG modified by (+) and (−) *anti*-BPDE, *Biopolymers* **24**, 2279 (1985).
40. B. E. Hingerty, R. H. Ritchie, T. L. Ferrell, and J. E. Turner, Dielectric effects in biopolymers: The theory of ionic saturation revisited, *Biopolymers* **24**, 427 (1985).
41. B. E. Hingerty, S. Figueroa, T. Hayden, and S. Broyde, Prediction of DNA structure from sequence: A build-up technique, *Biopolymers* **28**, 1195 (1989).
42. R. L. Jernigan and I. Bahar, Conformational search: Proteins, in *The Encyclopedia of Computational Chemistry*, edited by P. v. R. Schleyer, N. L. Allinger, T. Clark, J. Gasteiger, P. A. Kollman, H. F. Schaefer III, and P. R. Schreiner (Wiley, Chichester, 1998), Vol. 1, p. 563.
43. I. Kolossvary and W. C. Guida, Conformational analysis, 1, in *The Encyclopedia of Computational Chemistry*, edited by P. v. R. Schleyer, N. L. Allinger, T. Clark, J. Gasteiger, P. A. Kollman, H. F. Schaefer III, and P. R. Schreiner (Wiley, Chichester, 1998), Vol. 1, p. 513.
44. R. Kozack and E. L. Loechler, Molecular modeling of the conformational complexity of (+)-*anti* B[a]PDE-adducted DNA using simulated annealing, *Carcinogenesis* **18**, 1585 (1997).
45. R. Kozack and E. L. Loechler, Molecular modeling of the major adduct of (+)-*anti* B[a]PDE (N^2-dG) in the eight conformations and five DNA sequences most relevant to base substitution mutagenesis, *Carcinogenesis* **20**, 85 (1999).
46. R. Lavery, Nucleic acid conformation and flexibility: Modeling using molecular mechanics, in *The Encyclopedia of Computational Chemistry*, edited by P. v. R. Schleyer, N. L. Allinger, T. Clark, J. Gasteiger, P. A. Kollman, H. F. Schaefer III, and P. R. Schreiner (Wiley, Chichester, 1998), Vol. 3, p. 1913.
47. X. Liu, H. Yeh, J. Sayer, M. K. Lakshman, and D. M. Jerina, NMR solution structure of an undecanucleotide duplex with a complementary thymidine base opposite a 10R adduct derived from *trans* addition of a deoxyadenosine N^6-amino group to (−)-(7S,8R,9R,10S)-7,8-dihydroxy-9,10-epoxy-7,8,9,10-tetrahydrobenzo[a]pyrene, in preparation.
48. B. Mao, J. Chen, B. E. Hingerty, S. Amin, N. E. Geacintov, S. Broyde, and D. J. Patel, Conformation and 5′-intercalation of the aromatic BP residue in a (+)-*cis-anti*-[BP]-N^6-dA adduct opposite dT in a DNA duplex, *Proc. Am. Assoc. Cancer Res.* **37**, 118 (1996).
49. T. Meehan and K. Straub, Double-stranded DNA stereoselectively binds benzo[a]pyrene diol epoxides, *Nature* **277**, 410 (1979).
50. W. Olson, Spatial conformation of ordered polynucleotide chains. V. Conformational energy estimates of helical structure, *Biopolymers* **17**, 1015 (1978).

51. W. K. Olson and J. L. Sussman, How flexible is the furanose ring? A comparison of experimental and theoretical studies, *J. Am. Chem. Soc*. **104**, 270 (1982).
52. W. K. Olson and A. R. Srinivasan, Classical energy calculations of DNA, RNA and their constituents, in *Landolt-Bornstein Numerical Data and Functional Relationships in Science and Technology, Group VII. Biophysics Volume 1D*, edited by W. Saenger (Springer-Verlag, Berlin, 1990), p. 415.
53. R. Ornstein and R. Rein, Energetics of intercalation specificity. I. Backbone unwinding, *Biopolymers* **18**, 1277 (1979).
54. J. E. Page, B. Zajc, T. Oh-hara, M. K. Lakshman, J. M. Sayer, D. M. Jerina, and A. Dipple, Sequence context profoundly influences the mutagenic potency of *trans*-opened benzo[a]pyrene 7,8-diol 9,10-epoxide-purine nucleoside adducts in site-specific mutation studies, *Biochemistry* **37**, 9127 (1998).
55. D. Pearlman, D. Case, J. Caldwell, G. Seibel, U. C. Singh, P. Weiner, and P. A. Kollman, *AMBER 4.0 Documentation* (University of California, San Francisco, CA, 1986, 1991).
56. H. Pelletier, M. R. Sawaya, W. Wolfle, S. H. Wilson, and J. Kraut, Structures of ternary complexes of rat DNA polymerase β, a DNA template–primer, and ddCTP, *Science* **264**, 1891 (1994).
57. F. P. Perera, Environment and cancer: Who are susceptible? *Science* **278**, 1068 (1997).
58. J. L. Perrin, N. Poirot, P. Liska, C. Hanras, A. Theinpont, and G. Felix, Trace enrichment and HPLC analysis of PAHs in edible oils and fat products, using liquid chromatography on electron acceptor stationary phases in connection with reverse phase and fluorescence detection, in *Proc. 13th Int. Symp. Polynuclear Aromatic Hydrocarbons*, edited by P. Garrigues and M. Lamotte (Gordon and Breach, Langhorne, PA, 1993), p. 337.
59. L. M. Rice and A. T. Brunger, Torsion angle dynamics: Reduced variable conformational sampling enhances crystallographic structure refinement, *Proteins Struc. Func. Gen*. **19**, 277 (1994).
60. W. Saenger, *Principles of Nucleic Acid Structure* (Springer, Verlag, New York, 1984).
61. T. Schlick, B. E. Hingerty, C. Peskin, M. Overton, and S. Broyde, Search strategies, minimization algorithms and molecular dynamics simulations for exploring conformational spaces of nucleic acids, in *Theoretical Biochemistry and Molecular Biophysics*, edited by D. Beveridge and R. Lavery (Adenine Press, Schenectady, NY, 1990), p. 39.
62. T. Schlick, R. D. Skeel, A. T. Brunger, L. V. Kale, J. A. Board Jr., J. Hermans, and K. Schulten, Algorithmic challenges in computational molecular biophysics, *J. Comput. Phys*. **151**, 9 (1999).
63. E. J. Schurter, H. J. C. Yeh, J. M. Sayer, M. K. Lakshman, H. Yagi, D. M. Jerina, and D. G. Gorenstein, NMR solution structure of a nonanucleotide duplex with a dG mismatch opposite a 10R adduct derived from *trans* addition of a deoxyadenosine N^6-amino group to (−)-(7S,8R,9R,10S)-7,8-dihydroxy-9,10-epoxy-7,8,9,10-tetrahydrobenzo[a]pyrene, *Biochemistry* **34**, 1364 (1995).
64. E. J. Schurter, J. M. Sayer, T. Oh-hara, H. C. J. Yeh, H. Yagi, B. A. Luxon, D. M. Jerina, and D. G. Gorenstein, Nuclear magnetic resonance solution structure of an undecanucleotide duplex with a complementary thymidine base opposite a 10R adduct derived from *trans* addition of a deoxyadenosine N^6-amino group to (−)-(7R,8S,9R,10S)-7,8-dihydroxy-9,10-epoxy-7,8,9,10-tetrahydrobenzo[a]pyrene, *Biochemistry* **34**, 9009 (1995).
65. C. Simmerling, J. L. Miller, and P. A. Kollman, Combined locally enhanced sampling and particle mesh ewald as a strategy to locate the experimental structure of a nonhelical nucleic acid, *J. Am. Chem. Soc*. **120**, 7149 (1998).
66. S. B. Singh, B. E. Hingerty, U. C. Singh, J. P. Greenberg, N. E. Geacintov, and S. Broyde, Structures of the (+) and (−)-*trans-anti*-BPDE adducts to guanine-N^2 in a duplex dodecamer, *Cancer Res*. **51**, 3482 (1991).
67. S. B. Singh, W. A. Beard, B. E. Hingerty, S. H. Wilson, and S. Broyde, Interactions between DNA polymerase β and the major covalent adduct of the carcinogen (+)-*anti*-benzo[a]pyrene diol epoxide with DNA at a primer–template junction, *Biochemistry* **37**, 878 (1998).
68. T. J. Slaga, W. J. Bracken, G. Gleason, W. Levin, H. Yagi, D. M. Jerina, and A. H. Conney, Marked differences in the skin tumor-initiating activities of the optical enantiomers of the diastereomeric benzo[a]pyrene 7,8-diol-9,10-epoxides, *Cancer Res*. **39**, 67 (1979).
69. A. R. Srinivasan, N. Yathindra, V. S. R. Rao, and S. Trakash, Preferred phosphodiester conformations in nucleic acids: A virtual bond torsion potential to estimate lone-pair interactions in a phosphodiester, *Biopolymers* **19**, 165 (1980).

70. S. Vajda, Conformational Analysis; 2, in *The Encyclopedia of Computational Chemistry*, edited by P. v. R. Schleyer, N. L. Allinger, T. Clark, J. Gasteiger, P. A. Kollman, H. F. Schaefer III, and P. R. Schreiner (Wiley, Chichester, 1998), Vol. 1, p. 521.

71. K. H. Vousden, J. L. Bos, C. J. Marshall, and D. H. Philips, Mutations activating human C-Ha-rasI protooncogene (HRASI) induced by chemical carcinogens and depurination, *Proc. Natl. Acad. Sci. USA* **83**, 1222 (1986).

72. X. Wu and S. Wang, Self guided molecular dynamics simulation for efficient conformational search, *J. Phys. Chem. B* **102**, 7238 (1998).

73. X. Xie, N. E. Geacintov, and S. Broyde, Origin of opposite orientations in stereoisomeric DNA adducts derived from benzo[a]pyrene diol epoxide enantiomers with different tumorigenic potentials, *Biochem.* **38**, 2956 (1999).

74. H. J. C. Yeh, J. M. Sayer, X. Liu, A. S. Altieri, R. A. Byrd, M. K. Lakshman, H. Yagi, E. J. Schurter, D. G. Gorenstein, and D. M. Jerina, NMR solution structure of a nonanucleotide duplex with a dG mismatch opposite a 10S adduct derived from *trans* addition of a deoxyadenosine N^6-amino group to (+)-(7R,8S,9S,10R)-7,8-dihydroxy-9,10-epoxy-7,8,9,10-tetrahydrobenzo[a]pyrene: An unusual *syn* glycosidic torsion angle at the modified dA, *Biochemistry* **34**, 13570 (1995).

75. I. S. Zegar, F. R. Setayesh, B. L. DeCorte, C. M. Harris, T. M. Harris, and M. P. Stone, Styrene oxide adducts in an oligodeoxynucleotide containing the human N-*ras* codon 12 sequence: Structural refinement of the minor groove R(12, 2)- and S(12, 2)-α-(N^2-guanyl) stereoisomers from ^{1}H NMR, *Biochemistry* **35**, 4334 (1996).

76. I. S. Zegar, S. J. Kim, T. N. Johansen, C. M. Harris, T. M. Harris, and M. P. Stone, Adduction of the human N-*ras* codon 61 sequence with (−)-(7S,8R,9R,10S)-7,8-dihydroxy-9,10-epoxy-7,8,9,10-tetrahydrobenzo[a]pyrene: Structural refinement of the intercalated SRSR (61, 2) (−)-(7S,8R,9S,10R)-N^6-[10-(7,8,9,10-tetrahydrobenzo[a]pyrenyl]-2′-deoxyadenosyl adduct from ^{1}H NMR, *Biochemistry* **35**, 6212–6224.

77. R. H. Zhou and B. J. Berne, Smart walking—A new method for boltzmann sampling of protein conformations, *J. Comp. Phys*. **107**, 9185 (1997).